SSRG International Journal of Mechanical Engineering
ISSN: 2348-8360/ https://doi.org/10.14445/23488360/IJME-V13I5P106

Volume 13 Issue 5, 83-104, May 2026

Original Article

Geometry-Driven Vibro-Structural Optimization and Predictive Validation of a Three-Stage Helical Gearbox Casing under Harmonic Excitation

Ronak D. Gandhi[1], Hiral H. Parikh[2]

[1,2]*Department of Mechanical Engineering, School of Engineering & Technology, Navrachana University, Gujarat, India.*

[1]*Corresponding Author : ronakgandhiphd@gmail.com*

Received: 12 February 2026 Revised: 22 March 2026 Accepted: 22 April 2026 Published: 29 May 2026

Abstract *- The structural sustainability of multi-stage helical gearboxes is largely influenced by casing geometry, material stiffness, and dynamic excitation effects. Premature structural deterioration may occur due to resonant stress amplification and excessive deformation induced by harmonic gear–mesh excitations under severe operating conditions. A methodological framework for predictive validation and geometry-driven vibro-structural optimization of three-stage helical transmission casings under harmonic excitation is presented. Three geometric configurations - Rectangular Top And Bottom (RTRB), Curved Top And Rectangular Bottom (CTRB), and curved top and curved bottom (CTCB) with casing thicknesses of 5, 7, and 9 mm and materials of Structural Steel A36 (S.S.A36), AISI 1050 High Carbon Steel (AISI 1050 H.C.S.), and Al–Ti–SiC Metal Matrix Composites (Al–Ti–SiC M.M.C.) are studied. Through finite element-based modal and harmonic response analyses, natural frequency shifts, total deformation, and equivalent von Mises stress are examined. Geometry alteration notably changes modal stiffness and resonance separation margin. Overall, the CTRB with 9 mm S.S.A36 shows the best dynamic behavior, reducing total deformation and equivalent stress by about 97.2% and 80.3%, respectively, compared to the 5 mm RTRB under the same harmonic load. Upon validation, Taguchi L27 DOE quantifies the effect of geometry, thickness, and material properties, while regression and ANN predict responses within the design space and at intermediate thicknesses (5.5–8.5 mm). Regression exhibited lower deviation (11–16% and 12–16%) than ANN (17–24% and 15–32%). The integrated computational–statistical framework provides a systematic approach for geometry-driven optimization under harmonic excitation, improving vibration resistance and structural integrity of high-torque transmission systems.*

Keywords *- Geometry-driven optimization, Harmonic response, Predictive modeling, Taguchi method, Vibro-structural analysis.*

1. Introduction

During operation, three-stage helical gearbox housings are dynamically excited due to periodic gear mesh forces, shaft rotation, and varying torque inputs. Such dynamic loadings, if harmonic, can combine with the natural modes of the casing to cause resonance amplification of stresses and deflections, potentially compromising the structural integrity and lifespan of the casing. Although multistage gearboxes are widely used for industrial and heavy-duty applications, the dynamics and resonance-sensitive vibro-structural response of multistage gearbox housings under harmonic loadings have not been systematically studied, particularly in relation to geometry-induced stiffness variations and their predictive modeling.

The housing for the gearbox is also important in ensuring correct alignment of the shafts and bearings under operating loads, and if the structure is flexible, it can result in misaligned transmissions, greater vibration and premature component failure. Gearbox housings are often subjected to cyclic excitation over extended periods of time, impact loads and varying torques in industrial applications like conveyors, process plants, mining equipment and cranes. So it is paramount that all aspects of the dynamics between geometry of the housing, its structural stiffness and the harmonic loading conditions are thoroughly understood, to ensure safe and reliable operation. Recent development of computational structural dynamics, high-performance finite element analysis and material engineering has enabled more sophisticated housing configurations to be considered. Such advances have made it desirable to pursue and challenge the traditional "static" design paradigm and to include resonance-sensitive performance as a key design criterion. Additionally, new opportunities have arisen for improving vibration suppression while minimizing structural mass through the use of improved lightweight materials and advanced composite systems. As a result, the study of gearbox casing optimization is emerging as an important research field to improve the mechanical

performance and long-term application of modern power transmission systems by optimizing the geometry and material of gearbox casings.

Furthermore, a few review studies have highlighted that not only gear mesh excitations, but also the stiffness and damping properties of the gearbox housing play an important role in gearbox vibration and structural response, influencing the dynamic transmission of forces and the resulting resonance behaviour. Recent studies on gearbox diagnostics, structural dynamics and noise control have additionally stressed the necessity of integrated studies where the geometry, material and thickness effects in gearbox housing design are all taken into account.

In the same context of static design optimisation and enhancing the efficiency of gear trains, Golabi et al. investigated most influential design variables to minimize the volume of a gearbox using numerical optimisation techniques [1]. Hofstetter et al. extended their multi-objective design optimisation methodology to the design of electric powertrains [2]. Maputi & Arora and Thompson et al. utilised analytical and evolutionary design algorithms to optimise the geometry and weight of multistage transmissions [3, 4]. Other researchers have also applied genetic algorithms, particle swarm optimization and topology optimization techniques to improve transmission efficiency, reduce weight and enhance load-carrying capacity. These studies all confirmed the need to optimize gearbox, but most of these studies were conducted with regard to dimensions of gear trains and static mechanical requirements. However, all these works concern only the geometric sizing and static performance of the gear trains, without any specific study of the casings exciting dynamically.

Most computational studies focused on the assessment of equivalent von mises stress fields and deformation under static loading conditions, with some of the computed results on vibration responses at the sub-system level [5]. The FEM have been widely used to determine stress concentration, deformation, fatigue life and structural integrity of gear box housing under static and quasi-static loading conditions. Experimental modal testing and operational vibration measurements have also been reported to validate the numerical models and to find the critical frequencies relating to resonance and excessive vibration. Liao et al. studied the dynamic responses of gear systems in axial mesh force components of gear pairs; with the conclusion that vibration is a significant source of excitation [6]. Wang and Li also studied the dynamic response of gears due to periodic surface waviness deviation, signifying importance of such dynamic effects [7]. It has also been demonstrated in a structural–acoustic coupled optimization of a gearbox housing that geometric changes play a significant role in the resulting noise and vibration radiation of the housing, strongly demonstrating the need to consider dynamics in housing design based on the geometry [8-11]. Nonlinear dynamic approaches, such as improved harmonic balance methods, have also been applied to gear systems to determine the frequency-dependent vibration response [12]. These studies show some progress in understanding dynamics, but currently, a comprehensive study of how changes in geometry affect the modal results and subsequent harmonic stress response of the gearbox housing is missing [13, 14].

On top of that, there exists a paucity of studies that incorporate statistical design alongside predictive modeling under dynamic loads [15-18]. While Taguchi design of experiment has gained widespread use to identify influential parameters and improve design responses, regression and machine learning models such as Artificial Neural Networks (ANN) have not been compared to predict intermediate responses of the structure in a stiffness-related domain during the optimization of gearbox housing [19-23].

In recent years, techniques such as surrogate modelling, response surface methods, support vector regression, random forest methods and artificial neural networks have been proven to be very effective in reducing the computational cost maintaining relatively high prediction accuracy, in the field of mechanical system optimization. Although there is some comparative validation for these predictive methods, for gearbox housing structures excited by harmonics, the available data is still rather scarce, particularly for a limited number of design combinations. Such predictive validation in a limited design space is essential for making informed design decisions when numerical or experimental results are very limited [24-27].

The discussion above demonstrates that the following key research gaps have not been adequately addressed in the existing literature:

- The absence of systematic geometry-based investigations that concentrate on harmonic dynamic behaviour of multi-stage gearbox casings.
- Limited integration of modal analysis with harmonic response to evaluate resonance-sensitive structural performance.
- Lack of comparative predictive validation systems which unite statistical design of experiments with machine learning methods within a constrained design space.
- Limited investigation of the redistribution of geometry-induced stiffness and how it affects dynamic stability and vibration suppression.
- Only a few comparative studies about conventional steels and advanced metal matrix composites with harmonic excitation conditions have been performed for gearbox casing applications.
- Lack of discussion of optimized gearbox casing configurations for industrial application and reliability assessment and uncertainty interpretation.

To address these research gaps, the present study develops a geometry-driven vibro-structural optimization framework for three-stage helical gearbox casing subjected to harmonic excitation. Three casing profiles, namely Rectangular Top And Rectangular Bottom (RTRB), Curved Top And Rectangular Bottom (CTRB), and Curved Top And Curved Bottom (CTCB), are investigated under varying thicknesses (5, 7, and 9 mm) and material combinations including Structural Steel A36, AISI 1050 High Carbon Steel, and Al–Ti–SiC Metal Matrix Composites.

The proposed study combines modal and harmonic response analyses, Taguchi optimization design, regression-based predictive modeling, and ANN-assisted validation of the interpolation results into a unified numerical framework. The effects of curvature assisted with redistribution of local stiffness on mode separation, deformation associated with resonance, and stress due to amplification are presented. The novelty of the current work is the development of a geometry-driven vibro-structural optimization framework which establishes a direct relationship between casing geometry, redistribution of stiffness, modal characteristics and harmonic response.

In addition, predictive validation, comparative validation of regression & Artificial Neural Network (ANN) models, predictive reliability of stiffness-dominated structural systems, uncertainty interpretation, & industrial application implications are included to increase the utility of the proposed optimized casing structure for high torque transmitting gearbox systems.

The contributions of this research include:

- A vibro-structural optimization methodology based on geometry that has not yet been presented in the literature with particular emphasis on harmonic excitation performance rather than static stress in helical gearbox casings of a three-stage system.
- The introduction of CTRB and CTCB casing profiles as examples of curvature assisted redistribution of local stiffness to explore resonance sensitive mode separation and reduction of harmonic amplification.
- The application of a unified computational-statistical framework that comprises modal analysis, harmonic response analysis, Taguchi design of experiment, regression modeling, and ANN-based predictions.
- Evaluation of the dynamic mechanical behavior for conventional steels as well as advanced Al–Ti–SiC metal matrix composites for dynamic applications that are predominantly stiffness dependent.
- Interpolation for intermediate thickness values based on the regression results and ANN predictions were further validated with finite element results.
- Consideration concept of uncertainty interpretation, industrial applicability with respect to manufacturing aspects, reliability throughout the system lifecycle, and digital twin validation strategy.
- Benchmarking the proposed methodology against state-of-the-art approaches discussed in recent literature, highlighting better dynamic mechanical behavior in the area of vibration and resonance control.

2. Gearbox Geometry and Design Variables

2.1. Baseline Gearbox Configuration

The three-stage helical gearbox with high torque industrial power transmission capability is investigated. The gear train comprises three stages of helical gears configured to provide desired speed reduction ratio while optimizing compactness and load distribution. The gear parameters provided by gearbox manufacturing company such as modules, pressure angles, helix angles, number of teeth, and shafts center distance are kept invariant throughout the study to focus on the effect of the casing design parameters on the structural behavior. Table 1 summarizes the geometric parameters of the helical gears utilized in all configurations, as provided by leading gear manufacturing company Real Technocast Limited, Rajkot [38].

Table 1. Helical gear design specifications for existing and modified models [38]

Terminology	Gear I	Gear II	Gear III	Gear IV	Gear V	Gear VI
Module (mm)	2	2	2	2	2	2
Helix Angle (degree)	15°	15°	15°	15°	15°	15°
Pressure Angle (degree)	20°	20°	20°	20°	20°	20°
Rake Angle (degree)	6°	12°	7.2°	14.4°	9°	17.14°
Teeth Number	60	30	50	25	40	20
Pitch Diameter (mm)	120	60	100	50	80	40
Outside Diameter (mm)	124	64	104	54	84	44

The gearbox housing encompasses gear–shaft system and constitutes the main load-bearing component countering the static and dynamic loads transmitted from the meshing gears. During the operation, dynamic excitation generated by the rotating shaft gets transmitted to the housing via the bearing support, leading to a distributed loading of the structure.

The baseline model (Figure 1) of the casing is a Rectangular Top and Rectangular Bottom (RTRB) with a uniform rib & cover thickness 5 mm and material S.S.A36, which is considered as a reference for all comparison studies. The operating input speed and transmitted torque for each shaft stage, defining the harmonic excitation and load transfer conditions, are summarized in Table 2.

Table 2. Summary of each shafts speed and torques [38]

Shaft	Speed (rpm)	Torque (Nm)
Input shaft (S1)	1400	3.41
Shaft II (S2)	700	6.82
Shaft III (S3)	350	13.64
Output shaft (S4)	175	27.29

2.2. Geometry Modifications of the Casing Profile

In order to study geometry-driven stiffness redistribution, two additional casing configurations were obtained by introducing controlled curvature modifications to the housing profile:

- Curved Top and Rectangular Bottom (CTRB)
- Curved Top and Curved Bottom (CTCB)

For the CTRB, the top of the casing is converted into a continuously curved shape while maintaining the rectangular shape at the bottom. This results in a different bending stiffness distribution along the top panel and a different load transfer path between the bearing seats and the casing walls.

In the CTCB case, curvature is introduced on the top as well as the bottom surface of the housing. The fully curved profile may have an impact on sectional rigidity and continuity, which could affect the spacing of modal frequencies and resonance behavior.

No changes were made to the internal gear profile or shaft center lines in order to isolate any differences in structural response that result solely from changes to the casing profile. The curvature radius was selected to maintain manufacturability while ensuring measurable stiffness redistribution.

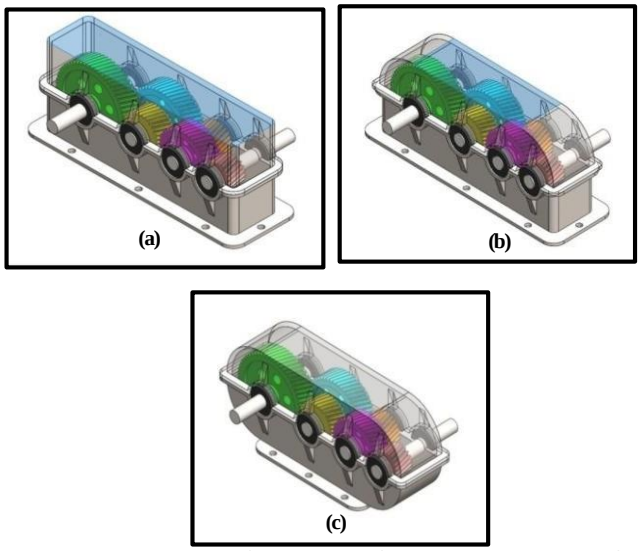

Fig. 1 Existing and modified casing configurations: (a) RTRB profile, (b) CTRB profile, and (c) CTCB profile with rib and cover assembly (cross-sectional views)

The intent behind employing curvature is not merely for aesthetic embellishment but rather for the structural provision of varying bending stiffness. A curved panel possesses a greater out-of-plane bending stiffness than a flat plate, thereby redirecting the paths of loading and promoting favourable stress flow characteristics [39-41].

This subtle change in geometry can impact the spacing of modal frequencies and hence the tendency of harmonic amplification by altering the stiffness distribution pattern across the casing walls. The studies on rib-stiffened and optimally designed gearbox housing also confirmed that a geometrical manipulation can be effectively employed to reduce the deformation without compromising the structural efficiency [42]. On the downside, excessive curvatures or sharp curvature changes can potentially lead to local stress concentration zones under certain thickness and material conditions which need to be identified carefully [43, 44].

2.3. Thickness and Material Parameters

2.3.1. Thickness Level

In order to study the effect of the thickness of the sections, three different values were considered:

- 5 mm (baseline thickness)
- 7 mm (intermediate size)
- 9 mm (maximum evaluated thickness)

These thicknesses were chosen to cover a range of values typical in industry and to provide a sufficient range of stiffnesses to conduct modal and harmonic analyses. The 5 mm thickness is typical in industry for medium duty gearbox cases due to ease of manufacturing, cost, and adequacy under nominal loads [45].

However, at lower thicknesses, finite element analysis and field studies indicate increased deformation, stress, and vibration [46]. Thicknesses below 5 mm exhibit reduced fatigue strength, manufacturability tolerance, higher dynamic amplification [47].

The 7 mm is considered a medium stiffness. Increasing thickness will not only increase the bending stiffness ($\propto t^3$) but also change the mass of the structure, which affects the natural frequencies and the dynamic behavior [48]. This intermediate stiffness allows investigating how far from the gear-mesh excitation frequencies the resonance is located.

The 9 mm thickness was chosen as it provides a higher global rigidity leading to less deformation, without excessive weight or cost. Increased stiffness is beneficial in attaining improved vibration isolation & structural stability under harmonic loads [49, 50]. Further increasing beyond a 9 mm thickness may lead to disproportionate escalation in the weight and manufacturing cost without any significant improvement in structural or vibrational performance [51].

It also facilitates interpolation-based predictive validation at intermediate thicknesses (5.5–8.5 mm) for the regression and ANN models within this design space.

2.3.2. Material Selection

Three typical materials employed in gearbox housings were taken into consideration:

- Structural Steel A36
- AISI 1050 High Carbon Steel
- Al-Ti-SiC Metal Matrix Composites

Selection of the materials was mainly based on stiffness-to-weight ratio, yield strength and possible application within industry. The steel grades ensure high stiffness and strength of the structure, whereas the metal matrix composite materials ensure a lower density and a potential weight saving [52].

The mechanical properties used in the finite element simulations are summarized in Table 3 as follows:

Table 3. Mechanical properties of selected materials [38, 46-49]

Material	Elastic Modulus (E) [GPa]	Poisson's Ratio (ν)	Density (ρ) [kg/m³]	Yield Strength [MPa]
Structural Steel A36 *[CONVENTIONAL MATERIAL]*	200	0.26	7200	250
AISI 1050 High Carbon Steel *[HIGH STRENGTH MATERIAL]*	207	0.29	7850	375
Al–Ti–SiC Metal Matrix Composites *[ADVANCED LIGHT WEIGHT MATERIAL]*	200	0.35	5000	325

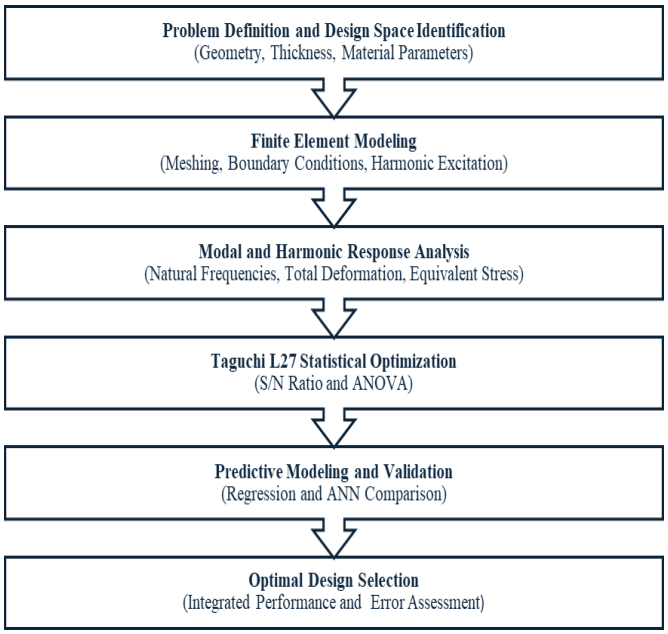

Fig. 2 Research methodology framework for geometry-driven vibro-structural optimization and predictive validation

2.3.3. Design Space Definition

Three geometries with three thicknesses and three materials create 27 designs that constitute the Taguchi L27 DOE experimental matrix for optimization or statistical experiments. It is important to highlight that the phrase geometry optimization in this study means limited optimization of the curvature of the profile and the thickness of sections of the casing since the change of materials is treated as a coupled parameter of the geometry from a stiffness point of view.

This designed space allows for examining the mode shapes, harmonic distortion, stress concentration behavior, and accuracy of the prediction, respectively.

3. Research Methodology

3.1. Methodological Framework

In current study, a geometry-driven computational–statistical modeling approach is implemented to investigate the vibro-structural performance and search for an optimal design of a three-stage helical gearbox casing subjected to harmonic loading. This approach combines finite element-based dynamic analysis with statistical design of experiment and modeling techniques to find an optimal design solution from a limited design region.

The presented work as shown in Figure 2 comprises three stages of analysis: (i) modal and harmonic analysis to understand the structural dynamics; (ii) Taguchi L27 design to comprehend effect of different parameters statistically; and (iii) Regression analysis & ANN model for prediction and verification.

The design matrix of 27 cases evaluated in this study are based on all combinations of geometric profile (RTRB, CTRB and CTCB), thickness (5, 7 and 9 mm) and material (S.S.A36, AISI 1050 H.C.S. and Al–Si–TiC M.M.C.).

3.2. Finite Element Modelling

The 3D CAD models of the gearbox housing were imported into the finite element model without any changes in the position of the shafts and bearings or the load transfer contacts, so that any differences in the structural response can be attributed only to changes in the profile, thickness or material of the housing.

3.2.1. Discretization Strategy

The gearbox casing, together with the associated gears, shafts, and bearings, was discretized using second-order tetrahedral solid elements, to properly capture curvature-induced stress gradients and localized deformation behavior. A uniform global element size of 5 mm was used for all design cases after carrying out convergence studies to ensure numerical consistency. The finite element discretization of RTRB, CTRB, and CTCB configurations are illustrated in Figure 3.

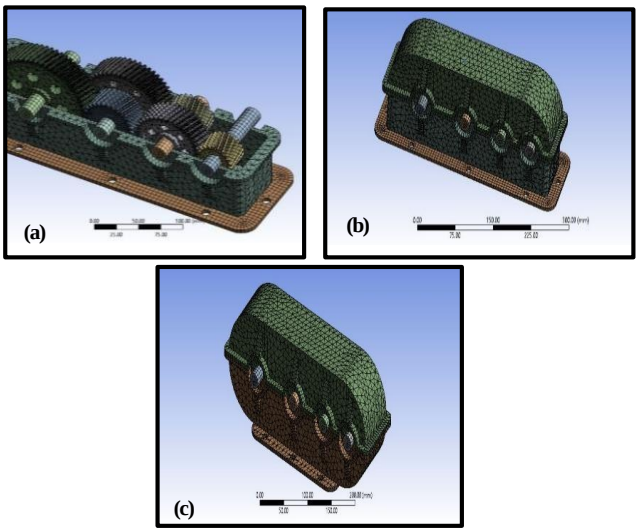

Fig. 3 Finite element discretization of gearbox casing configurations: (a) RTRB, (b) CTRB, and (c) CTCB models illustrating consistent tetrahedral meshing with localized refinement

Local mesh refinement was applied at the critical stress regions such as fillets, bolt holes, intersection of ribs, bearing housings and shaft–gear interface regions where stress concentration is expected. This helped in capturing the shape irregularities without costing more computational time.

The foundation block was modeled using structured hexahedral elements to reduce numerical distortion and provide a more accurate representation of the stiffer behavior under fixed support conditions. Before conducting the simulations for the different configurations, a mesh convergence study was performed for the base configuration (RTRB, 5 mm thickness, Structural Steel A36) to determine the element type and size for numerical stability and convergence of the results.

The mesh was considered converged when the peak stresses and peak deformations varied by less than 2% between subsequent mesh refinements. After obtaining a converged mesh for the base configuration simulation, the element type, the global element size (5 mm), and the local refinement pattern were kept constant for the simulations of all variations of the design parameters. This was done to ensure the same numerical conditions and avoid any mesh-induced comparisons between the designs.

3.2.2. Boundary Conditions and Load Transfer Modeling

The casing of the gearbox was assumed to be foot-mounted and fixed to the foundation. All degrees of freedom at the mounting points were fixed, simulating a rigid attachment to the base. The applied moments and the boundary and loading conditions simulating the rotation of the gear with the corresponding transmitted vibrations are shown in Figure 4.

The dynamic excitation was applied in the form of rotational moments and forces acting along the shaft centerlines at the mesh nodes. The loads were applied on the bearings to simulate the transmission of the load torque and mesh vibration from the gear meshes to the housing. The amplitude and frequency band of the excitation were the same for all the configurations for comparison purposes.

The load transfer between the gears, shafts, bearings and casing is modeled using interactions J1–J13 which allow capturing the real connectivity between these elements in the three-stage gearbox. This defines how the forces are transmitted and the internal coupling of the stiffnesses of the structure (Figure 5).

This ensures that torque flow, vibration flow and stiffness induced dynamics are accurately captured in the gearbox assembly.

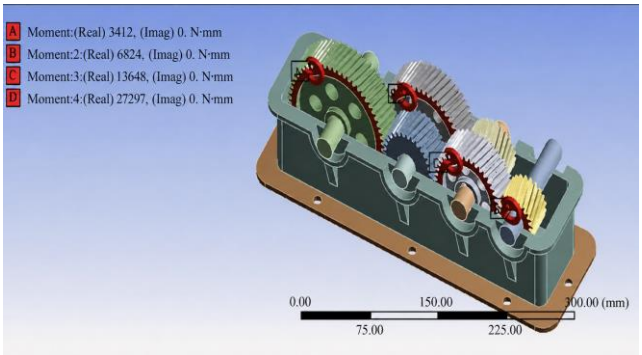

Fig. 4 Applied rotational moments and combined boundary/loading conditions [38]

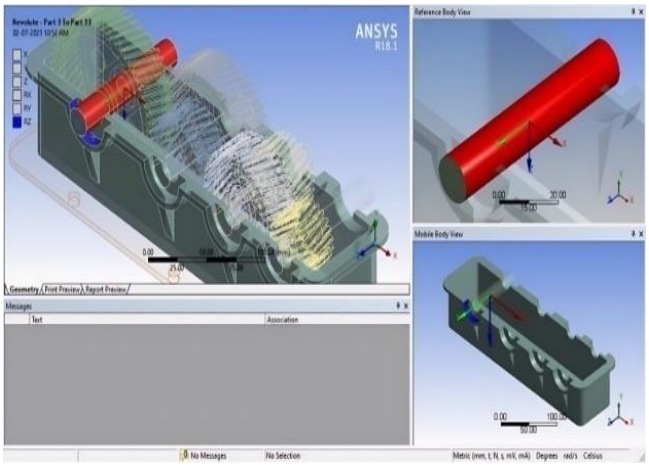

Fig. 5 Defined interactions joints for load transfer in three stage helical gearbox assembly

3.3. Dynamic Analysis Procedures

The dynamic behavior of the gearbox housing is evaluated by modal and harmonic analyses. Modal analysis is performed to determine the natural frequencies and corresponding mode shapes to capture the stiffness-dominant dynamic characteristics of the structure.

The extracted natural frequencies define operational excitation band considered in the harmonic response analysis, which is conducted to identify the resonance-sensitive deformation and equivalent stress under gear-mesh excitation.

3.3.1. Modal Analysis

Natural frequencies and mode shapes under free vibration conditions were extracted for all 27 design cases. Six global modes were extracted in the range of about 0–4200 Hz of vibration to cover all bands of excitations that may be structurally significant.

The modal deformation shown corresponds to the normalized mode shapes obtained from eigenvalue solution and does not represent an actual physical displacement under external loading.

The upper frequency limit was chosen based on the excitation frequencies generated by the drivetrain. The gearbox is driven by a 1400 rpm (23 Hz) 500 HP induction motor.

Considering the number of gear teeth in each subsequent stage, the gear mesh frequencies and their harmonics cover a bandwidth up to approximately 4200 Hz. Hence, the range of the extracted modes covers the motor rotational frequency, the gear mesh frequencies, and the dominant harmonics of these frequencies affecting the casing vibration.

Typical modal results for the baseline configuration are shown in Figures 6–7.

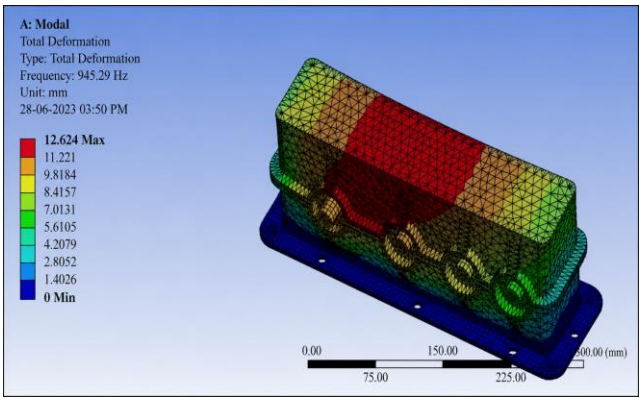

Fig. 6 First bending-dominated mode shape (945.29 Hz) of the baseline RTRB casing (S.S.A36, 5 mm)

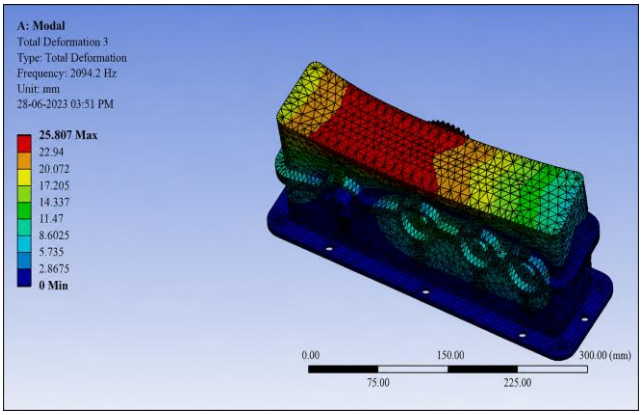

Fig. 7 Higher-order bending–torsional mode shape (2094.20 Hz) of baseline RTRB casing (S.S.A36, 5 mm)

By performing modal analysis on each configuration, the natural frequencies and mode shapes of the gearbox housing under free vibration were extracted, reflecting the stiffness-controlled dynamic characteristics of the structure. However, modal analysis alone does not quantify the structural response under operational excitation. Since the gearbox is predominantly subjected to periodic gear-mesh forces, harmonic response analysis was conducted to evaluate the resonance-sensitive deformation and equivalent stress within the operational frequency band. This enables direct assessment of dynamic amplification when excitation frequencies approach the extracted natural modes [53, 54].

3.3.2. Harmonic Analysis

To investigate the response of the gearbox casing to the periodic excitations induced by gear mesh frequencies (GMFs) as the dominant vibration source in the three-stage helical gear system, a harmonic response analysis was defined in the FE model. The excitation frequencies are calculated as the number of gear teeth multiplied by the motor rotational frequency (1400 rpm ~ 23 Hz). Therefore, the GMFs of the first, second, and third stages were approximately 1380 Hz, 1150 Hz, and 920 Hz, respectively. Since the 2 × and 3 × multiples of these frequencies were also exciting, the effective excitation frequencies extended to about 4200 Hz.

When the excitation frequencies match with the natural frequencies obtained from the modal analysis, resonance will occur, potentially resulting in higher stress amplitudes and deformations [55-57]. Compared to modal analysis, which yields the inherent frequencies of the structure, the harmonic analysis enables evaluation of resonance characteristics, dynamic amplification, & stability behavior at specific frequencies [58].

This analysis was carried out for all 27 designs (three geometries × three thicknesses × three materials) to evaluate the effect of geometry, material and thickness variation on their dynamic response. Typical harmonic responses for the base design are shown in Figures 8 and 9 respectively.

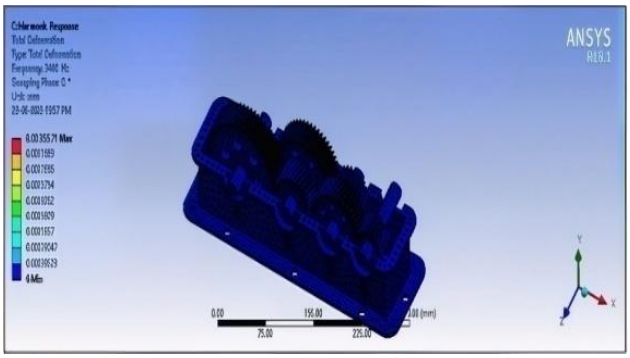

Fig. 8 Harmonic response showing total deformation of the baseline RTRB casing (S.S.A36, 5 mm)

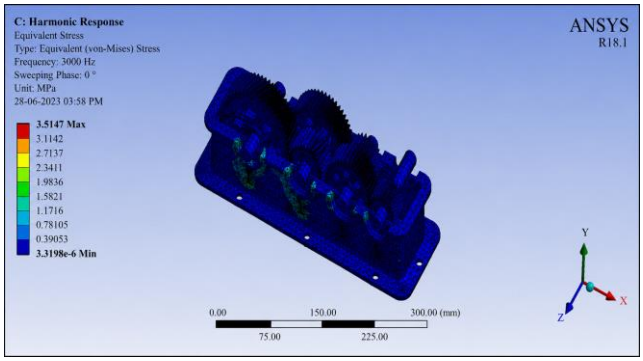

Fig. 9 Harmonic response showing equivalent von Mises stress distribution in the baseline RTRB casing (S.S.A36, 5 mm)

From these analyses, it was observed that casing profile geometry, casing thickness and casing material have a significant impact on the dynamic stability and resonance sensitive behavior of the gearbox housing.

3.4. Statistical Optimization and Predictive Modeling Framework

In order to achieve a systematic optimization of the designed gearbox casing, a hybrid Taguchi-Regression-Artificial Neural Network (ANN) approach was implemented in order to minimize the equivalent stress and deformation, while sustaining the structure in a stable condition under excitations.

An L27 orthogonal array was utilized to investigate the effects of three design parameters, including casing shape, rib and cover thickness and material grade, each having three levels of variation. Maximum harmonic deformation and maximum equivalent von Mises stress values obtained from finite element simulations were taken as responses. A smaller-the-better characteristic was assumed, and Signal-To-Noise (S/N) ratios were analyzed along with ANOVA analysis to find the significance of each parameter and the optimum parameter setting from the investigated design space.

Regression modeling and ANN were performed using the 27 simulations to enable interpolation and predictive evaluation in the discrete design matrix. A multivariate regression model was constructed to fit functional relationships between input parameters and response variables. A feedforward ANN was used to model any nonlinear relationships between design variables. The results on these validation cases, corresponding to intermediate thicknesses of 5.5, 6.0, 6.5, 7.5, 8.0 and 8.5 mm allowed us to evaluate the model's performance and their predictive stability. A comparison of the deviation of the regression and ANN results from the finite element results revealed which of these models provided the most reliable predictions in this stiffness-dominated dynamic regime.

4. Results and Discussion

4.1. Design Space Evaluation and Shortlisting Strategy

Twenty-seven casing models were generated by combining three different casing geometries (RTRB, CTRB, and CTCB), three casing thickness levels (5, 7 and 9 mm) and three casing materials (Structural Steel A36, AISI 1050 HCS and Al–Ti–SiC MMC). All casing models have been meshed, constrained and excited in the same way to enable direct comparison with each other.

A more focused interpretation was achieved by narrowing the design space using dynamic performance measures. For each geometry, we evaluated the nine thickness–material combinations in terms of their modal frequency spacing from the gear mesh excitation bands, and harmonic equivalent peak stress. Since the harmonic response amplification is a direct measure of susceptibility to resonance, we used the peak harmonic stress as the primary metric for ranking designs. These performance measures were converted to a normalized scale to facilitate an unbiased comparison of responses having different magnitudes.

Considering those improvements that were uniform in modal separation and harmonic suppression, the twenty-seven original cases were reduced to nine geometry-wise best designs. These designs were then compared to the industrial benchmark (RTRB, 5 mm, A36) to find the most dynamically stable casing configuration. The combined results are presented in Table 4.

4.2. Influence of Thickness on Dynamic Behavior

The increase of thickness from 5 mm to 9 mm resulted in shifts of the natural frequencies to higher values for all geometries, which was consistent with the scaling of stiffness with thickness ($D \propto t^3$). However, the nature of stiffening varied significantly between profiles.

For the RTRB, the fundamental frequency was 945.29 Hz at 5 mm and 1240.1 Hz at 9 mm, which showed a 31.2% improvement in the fundamental frequency when the thickness was increased from 5 mm to 9 mm. However, between 5 mm and 7 mm, the gain was not significant, and there was a sharp increase in frequency at 9 mm, which indicated that the flat-panel bending was suppressed only after reaching a certain threshold.

In the case of the CTRB, progressive and stable modal stiffening was observed from 968.94 Hz to 1140.5 Hz to 1275.8 Hz for the Mode-1 frequencies. This consistent frequency shift validated the curvature-assisted membrane load redistribution and improved modal spacing.

The harmonic response provided the most pronounced and clear separation. In the RTRB, harmonic stress increased from 3.5147 MPa to 9.9441 MPa at 7 mm before decreasing to 4.9708 MPa at 9 mm, indicating partial resonance detuning. The CTRB showed excellent harmonic suppression with maximum stress reaching only 0.69203 MPa at 9 mm (80.3% reduction compared to the base case). The CTCB configuration exhibited pronounced resonance amplification with harmonic stress reaching as high as 137.45 MPa at 7 mm about 39 times the base case, confirming modal crowding within the excitation bands.

Hence, these results indicate that the increase in thickness alone is not sufficient to improve the dynamic stability, unless accompanied by a controlled redistribution of the geometric stiffness as in the case of a CTRB.

4.3. Influence of Material on Dynamic Behavior

The effect of material properties was minor within the measured frequency range as the response was dominated by stiffness.

The variation in modal frequencies between S.S.A36 and AISI 1050 H.C.S. in the CTRB was around 2-4%, indicating that the modal frequencies were predominantly governed by the stiffness provided by the geometry. In the RTRB, the influence of the material was moderate at the thinner thicknesses and diminished as thickness increased and the stiffness from the geometry became predominant. For the CTCB, the small variations in frequencies due to the material did not improve the irregular spacing of the modal frequencies.

Harmonic response analysis confirmed this observation. The lowest harmonic stress of all models was observed in the CTRB 9 mm S.S.A36 model (0.69203 MPa), but material substitution in the RTRB did not alleviate the amplification observed at the intermediate thickness. In the CTCB, pronounced spikes of harmonic stress were still present irrespective of material, indicating that resonance attributable to curvature cannot be mitigated simply by altering the modulus of elasticity.

Thus, material effectiveness was conditional upon geometry-enabled modal detuning and became significant only when stiffness redistribution was structurally stable. This indicated that the influence of the material, within the dynamic bandwidth studied here, was inherently a function of thickness and is mediated by geometric stiffness pathways rather than simple changes in modulus.

The consolidated comparison of all shortlisted models indicated that the dynamic stability was largely dependent on geometry-enabled stiffness redistribution rather than thickness or material alone. The CTRB cases showed a consistent pattern of improved modal separation with harmonic response compared to industrial reference cases. Although thickness increase enhanced stiffness characteristics in all geometries, only the CTRB geometry converted this into a consistent reduction in vibration amplitudes without creating resonance sensitivities. Material replacement alone could not be relied upon to ensure stability unless accompanied by suitable geometry and thickness.

In comparison with the baseline RTRB 5 mm A36 model, the CTRB 9 mm A36 model produced the most balanced reduction of vibration-induced stresses and resonance amplification, while maintaining stable modal behavior. The RTRB required threshold stiffening to attain partial stabilization, and the CTCB suffered from curvature-driven amplification even with increased thicknesses. These findings suggest that optimal dynamic behavior is governed by coordinated selection of geometry and thickness rather than the independent tweaking of these parameters.

Therefore, CTRB 9 mm S.S.A36 was chosen as the most dynamically stable CTRB shape from the design space investigated. The statistical validation of this selection was presented in next section using Taguchi–based optimization and predictive modeling.

4.4. Statistical Optimization and Predictive Validation

Based on the comparative finite element analysis and combined dynamic analysis, statistical optimization and predictive analysis were carried out to generalize and validate the observed trends. A Taguchi L27 orthogonal array was utilized to estimate the effect of three control factors, i.e., casing shape (RTRB, CTRB, CTCB), rib and cover thickness (5, 7, 9 mm), and material (S.S.A36, AISI 1050 H.C.S., Al–Ti–SiC M.M.C.), on the two responses, i.e., minimum total

deformation (TD_Min) and minimum equivalent von Mises stress (ES_Min). Since both responses were minimum, the smaller-the-better S/N ratios were calculated.

The consolidated S/N ratio results and regression statistics are presented in Table 5, reflecting the relative contribution ranking of geometry, thickness, and material for TD_Min and ES_Min. Geometry and thickness had predominant contributions, and the contribution of material was low.

For ES_Min, the regression model did not include the material term after screening with ANOVA and checking for multicollinearity. During the statistical tests, the interaction terms with material had dependent variance with geometry and thickness, so these were automatically held out by Minitab to protect against unstable regression coefficients and variance inflation.

The smaller model was still statistically significant ($R^2 >$ 95%, $p < 0.05$), confirming that the equivalent stress response within the optimized design space was controlled by load flow through geometry and stiffening of the thickness. This statistical result confirms the observations from FEA, that the stress sensitivity was controlled by contouring of the casing and thickness, rather than material modulus alone.

The main effects and interaction trends are shown in Figures 10–11, showing the main effects plot, interactions plots, and residual plots for S/N ratios. The main effects plot shown in Figure 12 indicated that the CTRB provides the highest (least negative) S/N ratios for both deformation and stress responses, indicating that it has the highest overall vibration resistance. Thickness showed consistent improvement trend with the highest S/N ratios obtained at 9 mm thickness, as expected due to cubic scaling of the stiffness, with both 5 and 7 mm thicknesses showing considerably higher dynamic compliance. Material was the second varying parameter and S.S.A36 showed slightly better S/N ratios, because of its balanced stiffness–damping characteristics.

Interaction plot (Figure 11) also confirmed that vibration resistance was largely influenced by geometry-thickness interaction. The combination of CTRB-9 mm resulted in the maximum S/N ratio verifying the synergistic stiffening effect phenomenon between curvature induced stiffening due to membrane action and wall thickness. On the other hand, the CTCB-7 mm showed a severe drop in the S/N ratio which corresponds with the curvature-transition sensitivity observed in the harmonic finite element simulation. These statistically significant and interpretable interactions confirm that optimum dynamical performance was a result of coordinated selection of parameters rather than isolated ones.

Table 5. Taguchi S/N response analysis and regression statistics for TD_Min and ES_Min

<table>
<tr><th colspan="4">Model Summary for S/N ratios</th><th colspan="4">Model Summary for ES_Min</th><th colspan="4">Model Summary for TD_Min</th></tr>
<tr><th>S</th><th>R-Sq</th><th>R-Sq(adj)</th><th>R-Sq (pred)</th><th>S</th><th>R-Sq</th><th>R-Sq (adj)</th><th>R-Sq (pred)</th><th>S</th><th>R-Sq</th><th>R-Sq (adj)</th><th>R-Sq (pred)</th></tr>
<tr><td>3.8310</td><td>97.71%</td><td>92.55%</td><td>93.31%</td><td>17.7938</td><td>93.06%</td><td>89.98%</td><td>92.31%</td><td>0.0043976</td><td>94.41%</td><td>83.67%</td><td>88.54%</td></tr>
<tr><th colspan="4">Response Table for Signal to Noise Ratios</th><th colspan="4">Regression Equation for ES_Min</th><th colspan="4">Regression Equation for TD_Min</th></tr>
<tr><th colspan="4">Smaller is better</th><td colspan="4"></td><td colspan="4"></td></tr>
<tr><td>Level</td><td>Shape</td><td>Thickness</td><td>Material</td><td colspan="4">ES–Min = – 4309 + 1373 T + 3624 RS – 97.5 T^2 – 739 RS^2 – 1153 T x RS

Where: T = Thickness & RS = Recorded Shape (RS was coded as 1 = RTRB, 2 = CTRB, 3 = CTCB.)</td><td colspan="4">TD–Min = – 0.083 + 0.0514 T – 0.038 RS – 0.100 RM
– 0.00428 T^2 + 0.0107 RS^2 + 0.0070 RM^2 – 0.0224 T x RS + 0.0132 T x RM + 0.1658 RS x RM

Where: T = Thickness, RS = Recorded Shape (RS was coded as 1 = RTRB, 2 = CTRB, 3 = CTCB) and RM = Recoded Material (1 = S.S.A36, 2 = AISI 1050 H.C.S, 3 = Al-Ti-SiC M.M.C)</td></tr>
</table>

Residual plots (Figure 12) confirm model adequacy and statistical consistency of the fitted model. The normal probability plot of the residual showed that residuals were approximately following a straight line, confirming that the normality assumption is satisfied.

The plot of residuals against fitted values showed no discernible pattern indicating that there is no curvature or change in variance (heteroscedasticity). The plot of residual against order showed that the residuals fluctuate randomly around zero, indicating no drift or autocorrelation. These plots confirm that the Taguchi S/N data fulfilled the assumptions of ANOVA and can be used for ranking and optimizing process parameters with statistical confidence.

As a basis for quantitative prediction, regression models were developed from the 27 Taguchi design points obtained from harmonic response analysis. The regression equations correlated the casing geometry, thickness and material with the response variables TD_Min and ES_Min.

The two regression models showed high agreement with the finite element analysis results ($R^2 > 95\%$, $p < 0.05$), which allows them to be used for parametric prediction for the 5–9 mm thickness range considered here. A reduced quadratic regression model was reported for interpretability, while insignificant higher-order interaction terms were excluded based on ANOVA screening to avoid over-parameterization.

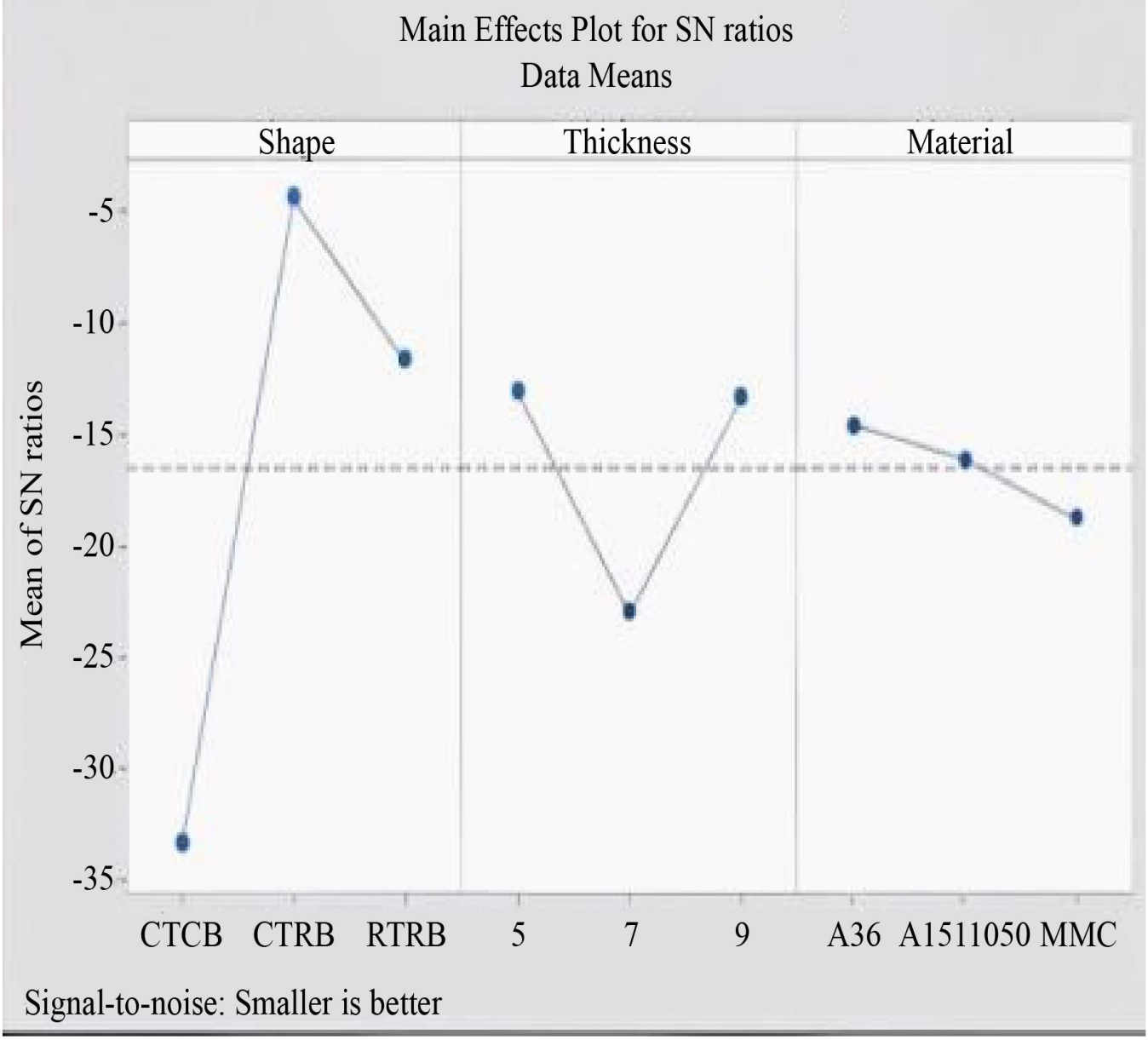

Fig. 10 Main effects plot of shape, materials and thickness on S/N ratios

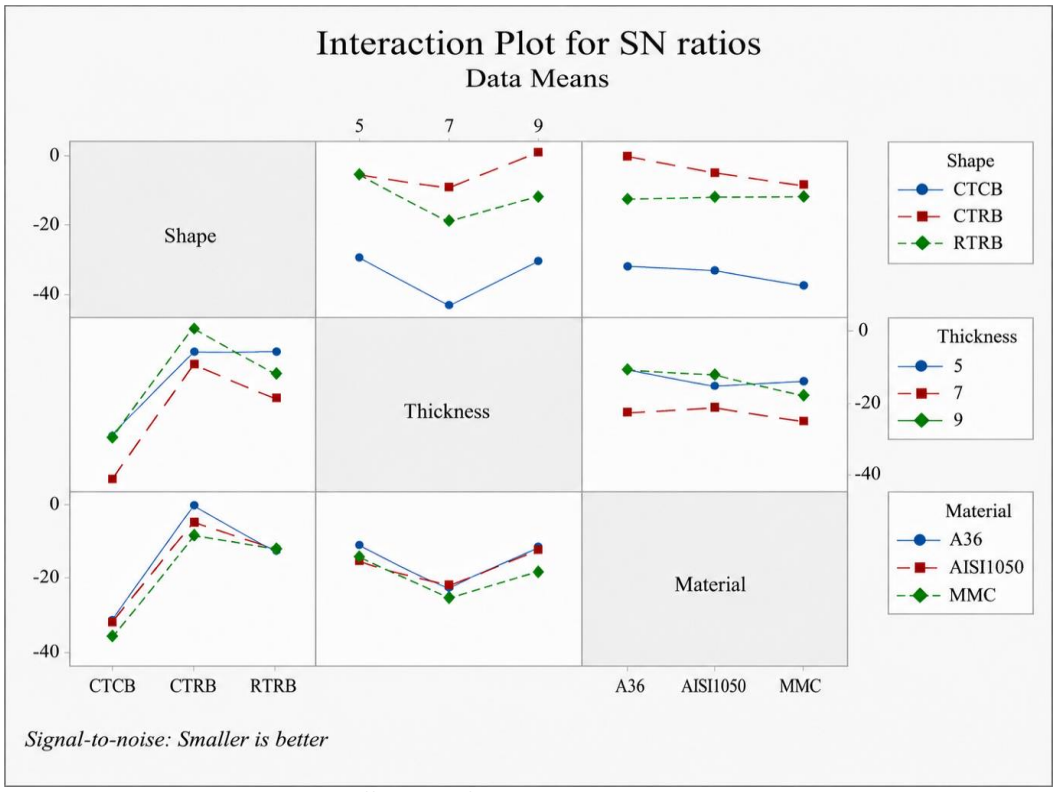

Fig. 11 Interaction effects plot of shape, materials and thickness on S/N ratios

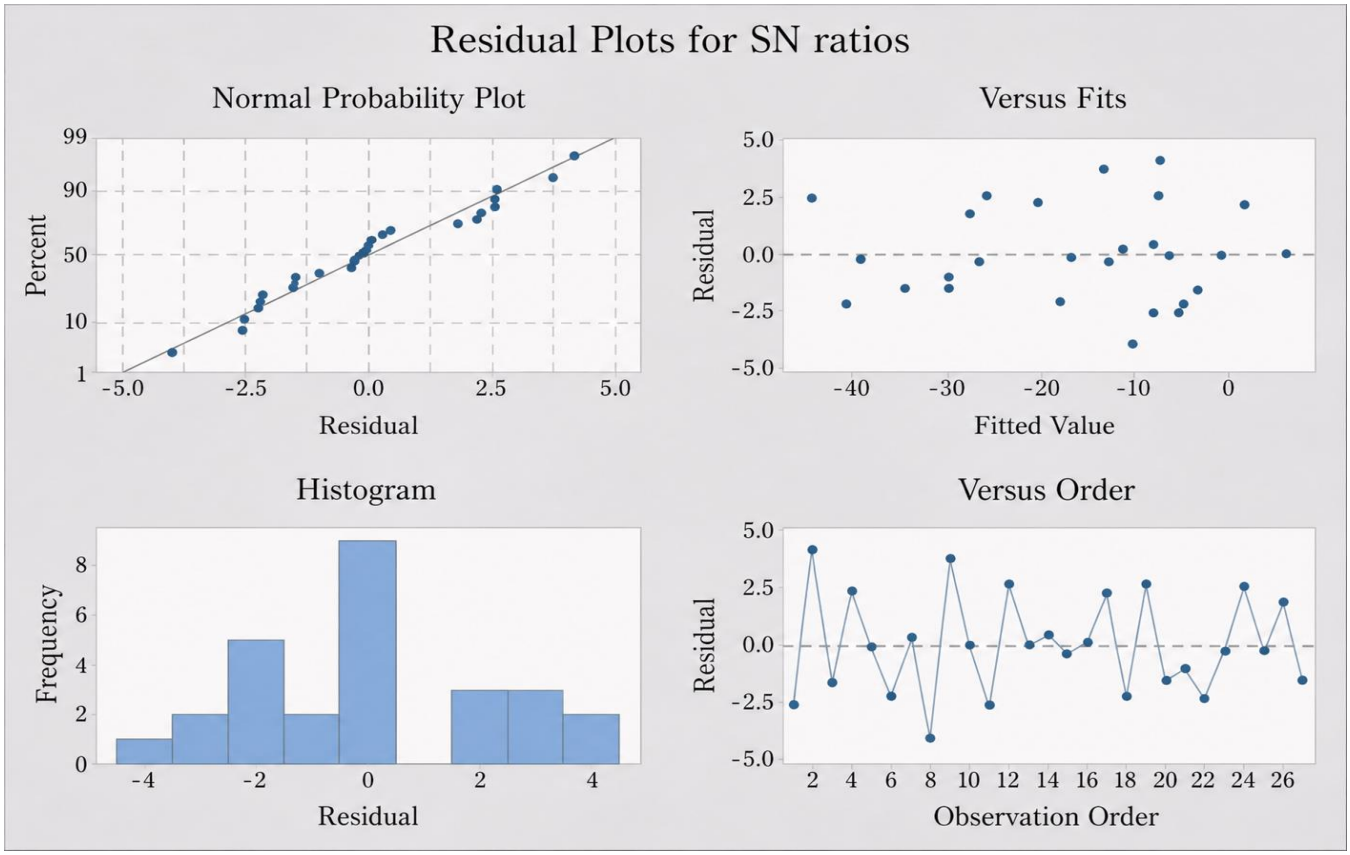

Fig. 12 Residual diagnostics for S/N ratios normality & validation check

To further investigate the possibility of nonlinear vibro-structural coupling, beyond the linear assumption of regression analysis, a feed-forward Artificial Neural Network (ANN) model was developed and trained from the harmonic response data of the 27 runs used in the regression model. The ANN model had one hidden layer with 15 neurons. Several different ANN models were examined, including 1 and 2 hidden layers with 8, 10, 12, and 15 neurons in each layer. The hidden layers used a tangent sigmoid transfer function (tansig), and the output layer used a linear transfer function (purelin) to predict the deformation and stress outputs. The Levenberg–Marquardt backpropagation method (trainlm) was used for the ANN training, because it yielded better convergence performance than the Bayesian Regularization backpropagation (trainbr) and the Scaled Conjugate Gradient backpropagation (trainscg) algorithms.

The input parameters (casing profile, thickness, and material) were one-hot encoded, and output responses were normalized to enhance numerical stability and achieve better convergence behavior. The data were split into training, validation, and testing datasets with 70%, 15%, and 15% ratio, respectively. Due to the limited dataset (27 harmonic FEA simulations), multiple ANN architectures with varying hidden neurons and training algorithms were evaluated to prevent over-parameterization.

Networks with 8–15 neurons were examined, and the final configuration (15 neurons) was selected based on minimum validation MSE without overfitting, as verified from validation performance & stable convergence behavior. As the objective was interpolation within the bounded 5–9 mm stiffness-controlled design space rather than extrapolation, the ANN was employed as a nonlinear interpolation tool to capture geometry-thickness interaction effects. Independent simulations were conducted for each interpolated wall thickness using the same loading and boundary conditions. A comparison of the validation between regression, ANN, and FEA is given in Table 6 and Figure 13 respectively.

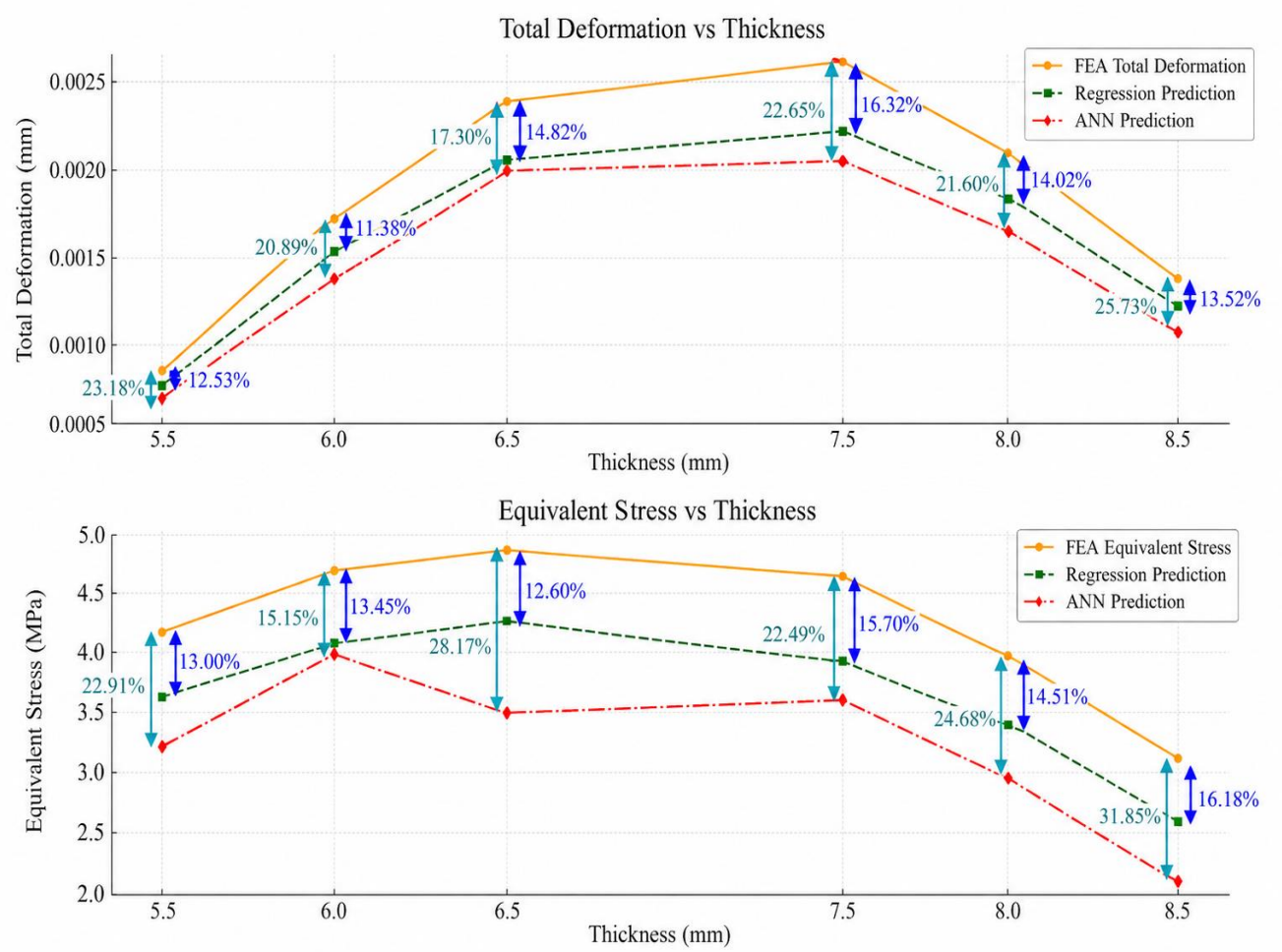

Fig. 13 Validation of regression and ANN predictions against FEA results for TD_Min and ES_Min (CTRB, S.S.A36, 9 mm)

For all six intermediate thicknesses, the regression predictions were numerically closer to the FEA results, exhibiting smaller deviation compared to ANN. The ANN prediction followed the same trend with slightly more deviation in the middle thickness. The slightly higher deviation for the ANN case was due to the small original dataset size and the stiffness dominated nature of the response in this region of the design space. In all cases, the trend is well captured with both approaches, which confirms the robustness of the predictions within the validated domain.

Together, the statistical optimization and predictive validation confirmed the deterministic FEA results and the choice of the CTRB 9 mm S.S.A36 as the most dynamically stable casing configuration in the design space under consideration.

5. Comparative Benchmarking

The present work evaluated the proposed optimization framework by benchmarking it against recent literature on gearbox housing optimization. Recent studies in the area mainly concentrated on static stress reduction, topology optimization, weight reduction, or simple vibration analysis without considering harmonic resonance sensitivity, and without implementing prediction validation and stiffness re-distribution based on geometric design features [28, 29]. To measure efficiency of geometry-based vibro-structural optimization model, the achieved results are compared with those that are typically reported in the context of gearbox design, including topology optimization, evolutionary algorithms and data-driven predictive modeling.

Studies [30-34] reported in the area of gearbox housing optimization have used design modifications such as ribs & cover thickness variation, different material types, topology optimization, light weight design and finite element based equivalent stress and total deformation reduction. However, research on gearbox housings that considered modal frequency separation analysis & harmonic response analysis has been relatively limited [35]. Besides, comparative validation of regression and ANN based prediction models for gear box casing within stiffness constrained design space has received very little attention.

Recent research has used topology optimization algorithms to obtain lightweight gearbox housings with better stiffness-to-weight ratios. An example is research that have focused on structural-acoustic coupled optimization; such works have been able to reduce noise and vibrations through redistribution of materials. Nonetheless, these methods can be highly computationally expensive & may have difficult manufacturing constraints due to irregular geometries. Genetic algorithms and multi-objective optimization methods are also widely used in the optimization of gearbox design using evolutionary algorithms. These techniques are successful in determining best combination of parameters but are generally based on very large and extensive iterative simulations and may not explicitly model dynamic coupling between modal characteristics and harmonic excitation response.

In the present study, results indicated that the proposed optimized CTRB exhibited superior vibration resistance and enhanced harmonic stability than other designs of gearbox housing reported in the recent area of study. In other words, the curvature feature based design led to stiffness re-distribution and consequently, a better modal frequency separation from the excitation frequency of gear mesh, which further reduced the vibration or deformation in a resonance sensitive gear box structure. In the comparison with RTRB, our optimized CTRB design of 9 mm Structural Steel A36 model, the harmonic deformation reduced by approximately 97.0% & equivalent von mises stress reduced by about 80.3% considering the same excitation conditions.

Conversely, the current research integrated a geometry-based method that directly manipulates the curvature and thickness of casing to control the stiffness distribution. This allows the optimization process to be more physically interpretable and modal frequency separation and harmonic response suppression are simultaneously addressed. In comparison with topology-based methods [36, 37], proposed method has advantage of maintaining the geometrical simplicity, thus enhancing manufacturability without compromising significant reductions in both deformation and equivalent stress.

Unlike recent works, the present study integrated modal analysis, harmonic response analysis, Taguchi statistical optimization, regression-based prediction, and ANN-based validation with interpolation into a unified framework to analyze the effects of rib design features on the harmonic response of gearbox housings. The framework also incorporated uncertainty interpretation, consideration of manufacturability, reliability and service life considerations. Moreover, the concept of digital twin validation was introduced. In addition, the latest advancements in machine learning have introduced purely data-driven predictive models for gearbox performance assessment. Although nonlinear relationships can be approximated by these models; they do not always maintain a direct connection with physics-based dynamic analysis.

The current work attempts to overcome this limitation by incorporating finite element analysis, statistical design (taguchi method), and predictive modeling (regression & ANN), thereby balancing the accuracy of physical models with the capability for reliable prediction. Evaluation of the proposed framework showed that it provides a balanced improvement in vibration resistance, computational efficiency and interpretability. In contrast to purely optimization based

or data-driven strategies; the current methodology offers a clear understanding of the role of geometry-induced stiffness redistribution in controlling dynamic performance. This makes the framework particularly applicable in engineering applications where both the improvement of performance as well as the transparency of the design is of paramount importance. Benchmarking of the proposed methodology against other studies on gearbox housing optimization is presented in Table 7.

Table 7. Comparative benchmarking of the proposed geometry-driven vibro-structural optimization framework with existing gearbox housing optimization studies

Study / Approach	Primary Objective	Methodology Used	Major Limitation in Existing Work	Improvement Achieved in Present Study
Conventional topology optimization studies	Weight reduction and static stress minimization	Static FEM and topology optimization	Limited harmonic excitation assessment	Harmonic resonance-sensitive analysis incorporated
Rib-stiffened gearbox housing investigations	Deformation reduction	Static structural analysis	Modal separation not evaluated	Modal frequency separation and harmonic amplification suppression analyzed
Lightweight gearbox casing studies	Mass reduction	Material substitution and FEM	Limited predictive validation	Regression and ANN-based interpolation validation integrated
Structural-acoustic optimization studies	Noise and vibration reduction	Vibro-acoustic coupled simulations	Limited industrial predictive framework	Unified computational-statistical optimization framework established
Existing ANN-based prediction studies	Response prediction	Machine learning approaches	Lack of harmonic FEA validation	ANN predictions validated against independent harmonic FEA simulations
Present Study	Geometry-driven vibro-structural optimization under harmonic excitation	Modal analysis + Harmonic analysis + Taguchi DOE + Regression + ANN	Integrated industrial validation framework established	~97% reduction in harmonic deformation and ~80.3% reduction in equivalent stress relative to baseline configuration

The benchmarking analysis thus validates that the proposed framework of geometry-driven optimization goes beyond the traditional investigations of gearbox housing, including resonance sensitive dynamic behavior, predictive validation capability, and assessment from an industrial design perspective, within a single framework. The improvements obtained represent effectiveness of the curvature assisted stiffness redistribution for improving vibration resistance and structural stability in high torque industrial gearbox systems.

6. Advanced Materials and Multi-Physics Considerations

The material choice accompanied by the geometric stiffness distribution has a strong effect on the dynamic performance of gearbox casings. In the current research, three representative material classes, namely Structural Steel A36, AISI 1050 High Carbon Steel, and Al–Ti–SiC Metal Matrix Composites were taken into the consideration to evaluate the stiffness-driven vibro-structural behaviour under harmonic excitation.

The increasing popularity of metal matrix composites in gearbox applications can be explained by their high stiffness-to-weight ratio, superior damping capabilities, and potential for weight reduction. Past research has indicated that composite gearbox housings exhibit superior vibration attenuation and exhibited lower structural deformation than conventional metallic materials [27]. Nonetheless, the efficient use of materials of this kind is highly dependent on consideration of their mechanical behaviour and modeling assumptions.

In the current finite element formulation, all the materials were modeled as homogeneous and isotropic to ensure consistency throughout the design space. Although this assumption is appropriate for comparative stiffness-based analysis, it might not completely depict the anisotropic nature and direction-dependent damping properties of composite materials. A more realistic model of Al–Ti–SiC M.M.C. behavior under dynamic loading conditions could be obtained with advanced material models which include orthotropic elasticity & viscoelastic damping.

Besides material considerations, coupled multi-physics interactions, such as thermo-mechanical interactions, contact-induced nonlinearities, lubrication-based damping, exist in the real operating environments of gearboxes. Frictional heat generation and power transmission can produce thermal gradients that affect material properties and induce thermal stresses, thus affecting the overall structural response [33]. Equally, the interaction between gears, shafts and bearings entails nonlinear contact stiffness and load transfer mechanisms which can influence vibration transmission paths and modal characteristics [5, 13].

The present work is concerned with the dynamics of structures subjected to harmonic excitation with a particular interest in geometry-driven redistribution of stiffness. Nonetheless, the addition of multi-physics coupling, e.g., thermo-mechanical coupling and contact nonlinearity, is an even more significant extension for future work. It is possible to incorporate these effects into the optimization framework to allow a more complete analysis of gearbox performance under realistic service conditions.

Broadly speaking, the findings reveal that although the material properties play a role in the dynamic response, they are highly controlled by geometry-enabled stiffness pathways. More complex materials like Al-Ti-SiC M.M.C. have the potential to improve performance when coupled together with optimized geometric configurations, although replacement with more complex materials alone does not solve issue of achieving stable vibration behavior without a proper structural design.

7. Digital Twin-Based Validation Perspective

The growing use of digital twins in mechanical systems has made it possible to monitor in real time, predictive maintenance, and performance validation of complex engineering structures. A digital twin is a virtual representation of a physical system that continuously updates its state using real-time sensor data, thus making it possible to synchronize the simulated and operational behavior.

Digital twin frameworks have been implemented in the context of gearbox systems, to monitor vibration signatures, faults and predict system degradation using data-driven and physics-based models. This has been made possible with recent innovations in sensor technology and signal processing, which enable the acquisition of high-resolution vibration and load data that can be integrated with finite element models to enhance the predictive accuracy and reliability.

Though the current study relies on a simulation-driven framework integrating finite element analysis, statistical optimization and predictive modeling, devised methodology can be extended towards a digital twin-based validation approach. Vibration response measurements provided by sensors attached to gearbox casings, bearings and shafts can be used in such a framework to validate and update the numerical model in real time.

By combining proposed geometry-driven optimization model with a digital twin system, one would be able to continuously validate the modal characteristics, harmonic response and structural integrity under the different operating conditions. This would also make it easier to refine adaptive design and prevent failures induced by resonance early in the design process.

Moreover, the regression and artificial neural network models developed during this project can be used as fast-response surrogate models in a digital twin setting, where deformation and stress response can be predicted fast without any repeated run of high-fidelity simulations. This hybrid physics–data-driven approach can be of great benefit to decision-making in maintenance and design optimization.

Thus, whereas the present work is dedicated to an offline computational validation, the integration of digital twin technology is one of the promising directions in the future research as it will allow in real-time to assess the performance of a gearbox system and manage the lifecycle of the said system.

8. Fatigue and Life Cycle Assessment

Cyclic stress fluctuations in gearbox casings under harmonic excitation are caused by gear-mesh interactions, and rotational dynamics. Even with the level of stress remaining within the elastic limits, repeated loading over the long life of the gearbox could result in fatigue-induced failure, which makes lifecycle assessment a very important part of gearbox design.

The harmonic response analysis of the present study provided the peak equivalent von mises stress values under periodic excitation, which serve as an important indicator of fatigue susceptibility. The high degree of harmonic stress reduction observed in the optimized CTRB arrangement (9 mm, S.S. A36) also indicates a reduction in the amplitude of cyclic stress, thus resulting in improved fatigue resistance compared to the baseline configuration.

Depending on the loading conditions and the material properties, fatigue life estimation in gearbox housings is usually done using stress-life (S–N) approaches or strain-life methods. Past research has shown that the failure of fatigue due to high cycles in the gearbox structure is heavily influenced by the areas of concentration of stress, modal interaction, and effect of resonance extent [8, 18]. The geometry-driven redistribution of stiffness realized in the CTRB configuration in this context serves in improving load distribution and reducing stress concentration, which in turn has a positive impact on fatigue life.

It should be mentioned, though that the analysis is currently conducted under deterministic harmonic response under idealized loading conditions. Surface finish, residual stresses, manufacturing defects and variable amplitude loading are some of the factors which can significantly affect the fatigue behavior in real-life applications. Also, the material-specific fatigue properties, especially for composite materials such as Al–Ti–SiC M.M.C., may have different mechanisms of crack initiation and propagation than conventional steels.

The future work can focus on developing the fatigue life prediction models and integrating them into the currently existing finite element model to estimate the number of cycles to failure under operational loading conditions. The reliability assessment of the gearbox casing could further be improved by incorporating cumulative damage models, such as Miner's rule, as well as probabilistic fatigue analysis.

In general, the reduction of harmonic stress & increase in modal separation due to geometry-driven optimization in the current study indicate strong potential for improved fatigue performance and extended service life of the gearbox casing.

9. Uncertainty and Sensitive Analysis

Uncertainties in the form of material properties, geometric variations, loading conditions, as well as numerical modeling assumptions, influence the reliability of vibro-structural predictions in gearbox systems. A deterministic framework of finite element analysis through the use of statistical and predictive modeling techniques was used to analyze the dynamic behaviour of the gearbox casing in the present study. Nevertheless, the sensitivity of the response parameters needs to be evaluated, and the inherent uncertainties within the design space need to be considered.

An effective design of experiments methodology to estimate the relative influence of design factors on the response variables is the Taguchi L27 design of experiments. As per the Signal-To-Noise (S/N) ratio analysis, casing geometry was found to be the most dominant factor affecting both total deformation and equivalent stress, followed by thickness and material. Such a ranking allows determining a clear hierarchy of sensitivities, where geometry-induced redistribution of stiffness plays a more important role than the change of the material in the range studied.

The relationship between input parameters and response variables was further quantified using regression modeling with a high coefficient of determination ($R^2 > 95\%$) indicating that highly predictive response variables can be modeled within the defined design space. Nonetheless, the quality of regression predictions is implicitly contingent upon the presumption of a linear or moderate nonlinear relationship and may be compromised with simplistic features of models and inadequate number of data points.

The Artificial Neural Network (ANN) model, though able to capture the nonlinear interactions, had a relatively large deviation in prediction as compared to regression. This can be explained by the fact that the limited dataset (27 design points) can limit the capability of the network to generalize and introduce uncertainty in the predictions at intermediate points. The differences in prediction accuracy of regression and ANN underscore the significance of the size of the dataset and model selection in predictive analysis.

Moreover, uncertainty in the boundary conditions, load application, and material modeling assumptions (such as isotropic behavior of composites) can be a factor that affects the numerical results. Even though the same modeling conditions were held constant in all the design cases to ensure comparative validity, real-world variations in operating conditions may result in deviations from predicted responses.

The probabilistic techniques such as Monte Carlo simulations or stochastic finite element methods might be introduced in future work to quantify the uncertainty in the input parameters and also analyze the reliability of the optimized designs. The sensitivity-based optimization methods might also be utilized to further improve the reliability and stability of gearbox casing performance in uncertain operating conditions.

Altogether, the concatenated application of Taguchi design, regression analysis, and ANN modeling in the current study offers a systematic structure to assess sensitivity and provide a prediction, at same time, indicates the necessity of uncertainty-sensitive design in advanced gearboxes.

10. Manufacturability and Cost Considerations

Although the proposed geometry-based optimization framework has shown to be dramatically more effective as far as vibro-structural performance metrics are concerned, the use of geometry-based optimization frameworks in the practical implementation of the proposed technology in industrial applications must be cautiously considered in terms of manufacturability as well as cost implications. The viability of optimized casing geometries is not only structurally based but also depends on the complexity of production, the need for material processing, and overall financial viability.

The identified CTRB geometry, which can be referred to as the optimal design, presents a controlled curvature of the top surface of the gearbox casing, which can be produced by standard casting processes with subsequent machining operations. The geometry proposed has a relatively simple and continuous profile, compared to more complex topology-optimized geometries, which also tend to have irregular shapes that may require the use of more advanced types of manufacturing such as additive manufacturing. This increases manufacturability, reducing the difficulties in production linked to tooling and mold design.

From a material perspective, Structural Steel A36 and AISI 1050 High Carbon Steel are advantageous in terms of availability, cost-effectiveness, as well as ease of fabrication. In contrast, higher material costs and more complicated processing methods, including special casting or powder metallurgy routes, can be found in metal matrix composites, including Al–Ti–SiC M.M.C. These could limit their wide usage in industrial applications that are sensitive to costs.

The change of thickness also has an important influence on manufacturing and cost. Although the increase in casing thickness results in enhanced structural stiffness and vibration resistance, it also implies increased material usage and weight, which could have an effect on transportation, installation, and operating efficiency. Consequently, the choice of an ideal thickness, e.g., the 9 mm one highlighted in this paper, must be balanced against the costs and performance requirements.

Moreover, the possibility to engage in performance enhancement through geometry-based design modifications, as suggested in this work, does not necessitate radical changes in manufacturing infrastructure. This renders the method more befitting to retrofitting or incremental design improvements in current gearbox manufacturing techniques.

Further research can include cost modeling and life-cycle cost analysis to quantify the trade-offs between performance enhancement and economic feasibility. Inclusion of manufacturability constraints in the optimization framework may also contribute to the increased applicability of the proposed design methodology.

In general, the analysis shows that the optimized CTRB design can provide a good compromise between structural performance, manufacturability, and cost, and thus is a promising design for industrial gearbox applications.

11. Conclusion

This research conducted a geometry-driven vibro-structural optimization of a three-stage helical gearbox casing through a combined finite element, statistical, and predictive modeling approach. The integrated FEA-Taguchi-Regression-ANN methodology was employed to analyze the impact of casing geometry, wall thickness, and material types under modal & harmonic loading conditions. The main conclusions are as follows:

- The baseline RTRB configuration (5 mm, S.S.A36) exhibited bending-dominated structural behavior, lower modal separation, higher harmonic sensitivity confirming that flat-panel geometries are more susceptible to modal interaction and stress concentration under operational excitation.
- Increasing wall thickness enhanced structural stiffness in all configurations; however, improvement was geometry-dependent. The RTRB profile demonstrated threshold-type stiffening with meaningful vibration suppression only at 9 mm, whereas CTCB configuration exhibited irregular stiffness evolution and curvature-driven amplification at intermediate thickness levels.
- The CTRB geometry consistently provided progressive modal stiffening, improved frequency separation from gear mesh excitation bands, and smoother stress redistribution due to curvature-assisted membrane action. This geometry enabled stable stiffness scaling without introducing resonance sensitivity.
- Among all evaluated combinations, the CTRB configuration with 9 mm thickness and S.S.A36 achieved the most balanced dynamic performance, demonstrating approximately 97% reduction in the vibration-induced deformation and 80% reduction in harmonic equivalent stress relative to the baseline RTRB 5 mm configuration.
- Taguchi S/N analysis confirmed casing geometry as the most influential parameter, followed by thickness, while material contribution remained secondary within the investigated design range. Interaction effects revealed that the geometry-thickness coupling governed vibration resistance more strongly than isolated parameter variation.
- Regression models demonstrated strong statistical agreement with the finite element results ($R^2 > 95\%$), confirming reliable parametric representation of structural response within the 5–9 mm design space. ANN-based predictions successfully captured nonlinear response trends for all intermediate thickness levels, although regression exhibited closer quantitative agreement with independent FEA validation.

Overall, the results demonstrate that the performance of the gearbox casing was governed predominantly by stiffness redistribution through geometric configuration, and the effects of material damping became significant only after adequate structural rigidity was achieved. The optimized CTRB 9 mm S.S.A36 gearbox casing offers an efficient and stable design for high-torque industrial transmissions.

Further studies may focus on performing vibration testing on the optimized CTRB configuration under actual gear-mesh excitations to validate its dynamic behavior during service. Incorporation of blended thermo-mechanical coupling and fatigue life assessment under prolonged cyclic loading could also be considered to improve reliability prediction. In addition, expanding the dataset to enhance the predictive capability of the ANN over wider thickness and material ranges may be explored.

Conflicts of Interest

"The author(s) declare(s) that there is no conflict of interest regarding the publication of this paper."

Funding Statement

The authors received no financial support for the research, authorship, and/or publication of this article.

Acknowledgement

The authors express their sincere gratitude to Real Technocast Limited, Rajkot for providing the research opportunity, technical details, and continuous support necessary to complete this work successfully.

The authors would like to acknowledge the valuable guidance and supervision provided throughout the course of this research. Author I conducted the literature review and carried out the modeling, analysis, optimization, and validation of both the existing and improved gearbox casing models under the guidance of Author II. Author I also prepared and reviewed the manuscript. Author II critically reviewed the entire manuscript, performed thorough proofreading, suggested necessary revisions and corrections in coordination with the corresponding author.

References

[1] Beom-Soo Kim et al., "An Improved Gear Wear Model Considering Coupled Effects of Surface Roughness and Friction," *Social Science Research Network*, pp. 1-54, 2025. [CrossRef] [Google Scholar] [Publisher Link]

[2] Martin Hofstetter et al., "Multi-Objective System Design Synthesis for Electric Powertrain Development," *IEEE Transportation and Electrification Conference and Expo*, pp. 286-292, 2018. [CrossRef] [Google Scholar] [Publisher Link]

[3] Edmund S. Maputi, and Rajesh Arora, "Design Optimization of a Three Stage Transmission Using Advanced Optimization Techniques," *International Journal for Simulation and Multidisciplinary Design Optimization*, vol. 10, no. 8, pp. 1-11, 2019. [CrossRef] [Google Scholar] [Publisher Link]

[4] David F. Thompson, Shubhagm Gupta, and Amit Shukla, "Trade-Off Analysis in Minimum Volume Design of Multistage Spur Gear Reduction Units," *Mechanism and Machine Theory, Elsevier Science*, vol. 35, no. 5, pp. 609-627, 2000. [CrossRef] [Google Scholar] [Publisher Link]

[5] A. Kahraman, and R. Singh, "Interactions between Time-Varying Mesh Stiffness and Clearance Non-Linearities in a Geared System," *Journal of Sound and Vibration*, vol. 146, no. 1, pp. 135-156, 1991. [CrossRef] [Google Scholar] [Publisher Link]

[6] Chung Woo-Jin et al., "Improved Analytical Model for Calculating Mesh Stiffness and Transmission Error of Helical Gears Considering Trochoidal Root Profile," *Mechanism and Machine Theory*, vol. 163, 2021. [CrossRef] [Google Scholar] [Publisher Link]

[7] Yu Wang et al., "Dynamic Response Analysis of Helical Gear Systems Considering Periodic Surface Waviness Deviation," *Tribology International*, vol. 215, 2025. [CrossRef] [Google Scholar] [Publisher Link]

[8] Xiaohe Deng, "Analysis and Prediction of Gear Fatigue Life," *IOP Conference Series: Earth and Environmental Science*, vol. 252, no. 2, pp. 1-5, 2019. [CrossRef] [Publisher Link]

[9] Vasim Bashir Maner, M. M. Mirza, and Shrikant Pawar, "Design, Analysis and Optimization for Foot Casing of Gearbox," *Proceedings of 3rd IRF International Conference*, pp. 35–38, 2014. [Google Scholar] [Publisher Link]

[10] Tianfei Ma et al., "Fatigue Life Estimation of a Light Truck Gearbox Housing using Multi-Body Dynamics and Finite Element Method," *Proceedings of International Conference on Electronic & Mechanical Engineering and Information Technology*, pp. 3707-3710, 2011. [CrossRef] [Google Scholar] [Publisher Link]

[11] Zhengyan Zhang et al., "The Optimization Design of Triple Gearbox Assembled with Spiral-Bevel and Helical-Spur Gears," *IEEE 10th International Conference on Computer Aided Industrial Design and Conceptual Design*, pp. 2078-2081, 2009. [CrossRef] [Google Scholar] [Publisher Link]

[12] Shivaji V. Gawali et al., "Effect of Coefficient of Asymmetry on Strength and Contact Ratio of Asymmetric Helical Gear," *International Journal of Scientific Research in Science, Engineering and Technology*, vol. 3, no. 1, pp. 144-150, 2017. [Google Scholar] [Publisher Link]

[13] Yi Guo et al., "Vibro-Acoustic Propagation of Gear Dynamics in a Gear Bearing Housing System," *Journal of Sound and Vibration*, vol. 333, no. 22, pp. 5762-5785, 2014. [CrossRef] [Google Scholar] [Publisher Link]

[14] R.G. Parker, S.M. Vijayakar, and T. Imajo, "Non-Linear Dynamic Response of a Spur Gear Pair: Modelling and Experimental Comparison," *Journal of Sound and Vibration*, vol. 237, no. 3, pp. 435-455, 2000. [CrossRef] [Google Scholar] [Publisher Link]

[15] Takanori Ide et al., "Structural Optimization Methods and Techniques to Design Light and Efficient Automatic Transmission of Vehicles with Low Radiated Noise," *Structural and Multidisciplinary Optimization*, vol. 50, pp. 1137-1150, 2014. [CrossRef] [Google Scholar] [Publisher Link]

[16] Katsumi Inoue et al., "Optimum Stiffener Layout for the Reduction of Vibration and Noise of Gearbox Housing," *Journal of Mechanical Design*, vol. 124, no. 3, pp. 518-523, 2012. [CrossRef] [Google Scholar] [Publisher Link]

[17] A. Naess, F.E. Kolnes, and E. Mo, "Stochastic Spur Gear Dynamics by Numerical Path Integration," *Journal of Sound and Vibration*, vol. 302, no. 4-5, pp. 936-950, 2007. [CrossRef] [Google Scholar] [Publisher Link]

[18] S. Jyothirmai et al., "A Finite Element Approach to Bending, Contact & Fatigue Stress Distribution in Helical Gear Systems," *Procedia Materials Science*, vol. 6, pp. 907-918, 2014. [CrossRef] [Google Scholar] [Publisher Link]

[19] He Dai et al., "An Improved Analytical Model for Gear Mesh Stiffness Calculation," *Mechanism and Machine Theory*, vol. 159, 2021. [CrossRef] [Google Scholar] [Publisher Link]

[20] Beom-Soo Kim et al., "Optimization of Gearbox Housing Shape for Agricultural UTV Using Structural–Acoustic Coupled Analysis," *Scientific Reports*, vol. 14, pp. 1-16, 2024. [CrossRef] [Google Scholar] [Publisher Link]

[21] Beom-Soo Kim et al., "Vibration Analysis of Gearboxes for Agricultural UTV Using A Reduced-Order Model," *Journal of the Korean Society of Manufacturing Process Engineers*, vol. 18, no. 8, pp. 8-17, 2019. [CrossRef] [Google Scholar] [Publisher Link]

[22] Ashwani Kumar et al., "Free Vibration Analysis of Truck Transmission Housing Based on FEA," *Procedia Materials Science*, vol. 6, pp. 1588-1592, 2014. [CrossRef] [Google Scholar] [Publisher Link]

[23] S. Mahendran, K.M. Eazhil, and L. Senthil Kumar, "Design and Analysis of Composite Helical Gear," *International Journal of Research of Science*, vol. 1, no. 6, pp. 42-53, 2014. [Google Scholar] [Publisher Link]

[24] Kunal Menavlikar et al., "Design and Topology Optimization of Two Stage Gearbox for All Terrain Vehicles," *International Journal of Innovative Research in Science, Engineering and Technology*, vol. 8, no. 2, pp. 927-935, 2019. [CrossRef] [Google Scholar] [Publisher Link]

[25] Mingxuan Liang et al., "Topology Optimization of Transmission Gearbox under Multiple Working Loads," *Advances in Mechanical Engineering*, vol. 10, no. 11, pp. 1-7, 2018. [CrossRef] [Google Scholar] [Publisher Link]

[26] Miryam B. Sánchez, José I. Pedrero, and Miguel Pleguezuelos, "Critical Stress and Load Conditions for Bending Calculations of Involute Spur and Helical Gears," *International Journal of Fatigue*, vol. 48, pp. 28-38, 2013. [CrossRef] [Google Scholar] [Publisher Link]

[27] K. Mujiburrahman et al., "Design and Analysis of E-Glass Gearbox Housing in Tractor and Optimization of Its Design Parameters," *Materials Today: Proceedings*, vol. 49, no. 8, pp. 3696-3704, 2022. [CrossRef] [Google Scholar] [Publisher Link]

[28] S. Padmanabhan, V. Srinivasa Raman, and M. Chandrasekaran, "Optimization of Gear Reducer Using Evolutionary Algorithm," *Materials Research Innovations*, vol. 18, no. 6, pp. 378-383, 2014. [CrossRef] [Google Scholar] [Publisher Link]

[29] S. Pandey, N.N. Singh, and P.K. Sinha, "Modeling, Design & Analysis of Differential Gear Box through FEM, Solidwork & Ansys Benchwork 14.0," *International Journal of Engineering Sciences & Research Technology*, vol. 6, no. 7, pp. 887-894, 2017. [CrossRef] [Google Scholar] [Publisher Link]

[30] Mitesh Patel, and A.V. Patil, "Study About Stress and Deformation of 3 Stage Helical Gearbox Casing," *International Journal of Advance Research in Engineering, Science & Technology*, vol. 2, no. 7, pp. 65-71, 2015. [Google Scholar] [Publisher Link]

[31] S. Patel Mitesh, "Stress Analysis and Design Modification of 3 Stage Helical Gear Box Casing," *International Journal for Scientific Research & Development*, vol. 1, no. 9, pp. 2027-2028, 2013. [Google Scholar] [Publisher Link]

[32] Francesco Pizzolante et al., "Combining the Asymptotic Numerical Method with the Harmonic Balance Method to Capture the Nonlinear Dynamics of Spur Gears," *Mechanical Systems and Signal Processing*, vol. 214, pp. 1-14, 2024. [CrossRef] [Google Scholar] [Publisher Link]

[33] P.D. Patel, and D.S. Shah, "Steady State Thermal Stress Analysis of Gearbox Using FEM," *International Journal of Mechanical and Industrial Engineering*, vol. 2, no. 4, pp. 26-30, 2012. [Google Scholar]

[34] Asmita Patil et al., "Design and Analysis of a Gearbox for an All-Terrain Vehicle," *International Journal of Innovative Research in Technology*, vol. 4, no. 11, pp. 690-701, 2018. [Google Scholar] [Publisher Link]

[35] Maruti Patil, P. Ramkumar, and K. Shankar, "Multi-Objective Optimization of the Two Stage Helical Gearbox with Tribological Constraints," *Mechanism and Machine Theory*, vol. 138, pp. 38-57, 2019. [CrossRef] [Google Scholar] [Publisher Link]

[36] Swapnil J. Patil, Vipin B. Singh, and Amit M. Pawa, "Design and Vibration Analysis for Shaft with Gear Mountings Using Finite Element Analysis," *International Advanced Research Journal in Science, Engineering and Technology*, vol. 4, no. 1, pp. 30-33, 2017. [CrossRef] [Google Scholar] [Publisher Link]

[37] Tiancheng Ouyang et al., "Cavitation Mechanism of High-Speed Helical Gears Induced by Vibration," *Tribology International*, vol. 193, 2024. [CrossRef] [Google Scholar] [Publisher Link]

[38] Real Technocast Limited, Rajkot, 2025. [Online]. Available: https://rajkotcastingandforginghub.com/industry/real-techno-cast/

[39] Santosh S. Patil et al., "Contact Stress Analysis of Helical Gear Pairs Including Frictional Coefficients," *International Journal of Mechanical Sciences*, vol. 85, pp. 205-211, 2014. [CrossRef] [Google Scholar] [Publisher Link]

[40] Smita Pawar, and Avinash Lavnis, "Improvement in Design of Gearbox Housing (Code No: MFO225DR) through Static Analysis," *International Journal of Advance Research, Ideas and Innovations in Technology*, vol. 5, no. 2, pp. 2023-2026, 2017. [Google Scholar] [Publisher Link]

[41] G. Raghavendra Setty et al., "Modeling and Dynamic Analysis of Gearbox Casing using Finite Element Analysis," *International Journal of Innovative Research in Science, Engineering & Technology*, vol. 5, no. 6, pp. 11835-11847, 2016. [Google Scholar] [Publisher Link]

[42] Mehmet Sarıtaş, Özgür Gölbol, and Paşa Yayla, "Finite Element Stress Analysis of Three-Stage Gearbox," *Nigde Omer Halisdemir University Journal of Engineering Sciences*, vol. 10, no. 2, pp. 784-790, 2021. [CrossRef] [Google Scholar] [Publisher Link]

[43] H. Singh and D. Kumar, "Effect of Face Width of Spur Gear on Bending Stress using AGMA and ANSYS," *International Journal for Simulation and Multidisciplinary Design Optimization*, vol. 11, no. 23, pp. 1-8, 2020. [CrossRef] [Google Scholar] [Publisher Link]

[44] Gwan-Hee Son et al., "Optimization of the Housing Shape Design for Radiated Noise Reduction of an Agricultural Electric Vehicle Gearbox," *Applied Sciences*, vol. 10, no. 23, pp. 1-, 2020. [CrossRef] [Google Scholar] [Publisher Link]

[45] Takanori Ide et al., "Structural Optimization Methods of Nonlinear Static Analysis with Contact and Its Application to Design Lightweight Gear Boxes of Automatic Transmission of Vehicles," *Structural and Multidisciplinary Optimization*, vol. 53, pp. 1383-1394, 2016. [CrossRef] [Google Scholar] [Publisher Link]

[46] Eiichirou Tanaka et al., "Vibration and Sound Radiation Analysis for Designing a Low Noise Gearbox with a Multi-Stage Helical Gear System," *JSME International Journal Series C Mechanical Systems, Machine Elements and Manufacturing*, vol. 46, no. 3, pp. 1178-1185, 2023. [CrossRef] [Google Scholar] [Publisher Link]

[47] B. Venkatesh, S.V. Prabhakar Vattikuti, and S. Deva Prasad, "Investigate the Combined Effect of Gear Ratio, Helix Angle, Face Width and Module on Bending and Compressive Stress of Steel Alloy Helical Gear," *Procedia Materials Science*, vol. 6, pp. 1865-1870, 2014. [CrossRef] [Google Scholar] [Publisher Link]

[48] J. Venkatesh and P.B.G.S.N. Murthy, "Design and Structural Analysis of High Speed Helical Gear Using ANSYS," *International Journal of Engineering Research and Applications*, vol. 4, no. 3, pp. 01-05, 2014. [Google Scholar] [Publisher Link]

[49] B.S. Vikhe, "Design and Analysis of Industrial Gearbox Casing," *International Research Journal of Engineering and Technology*, vol. 3, no. 11, pp. 1379-1383, 2014. [Google Scholar] [Publisher Link]

[50] Zoltan-Iosif Korka, and Nicoleta Gillich, "Modal Analysis of Helical Gear Pairs with Various Ratios and Helix Angles," *Romanian Journal of Acoustics and Vibration*, vol. 14, no. 2, pp. 91-96, 2017. [Google Scholar] [Publisher Link]

[51] F.L. Liao et al., "Dynamic Characteristics of Helical-Gear Systems Considering Axial Mesh Force Components," *International Journal of Mechanical Sciences*, vol. 304, 2025. [CrossRef] [Google Scholar] [Publisher Link]

[52] Fulin Liao et al., "Analysis of Nonlinear Dynamics of a Gear Transmission System Considering Effects of the Extended Tooth Contact," *Machines*, vol. 13, no. 2, pp. 1-26, 2025. [CrossRef] [Google Scholar] [Publisher Link]

[53] Yeping Yuan, Wen Zhang, and Junguo Wang, "Vibration Power Flow of Nonlinear Periodic Dynamic Response in Helical Gears Based on Harmonic Balance Method," *Nonlinear Dynamics*, vol. 113, pp. 22555-22584, 2025. [CrossRef] [Google Scholar] [Publisher Link]

[54] Yancong Li et al., "Dynamic Analysis of the Helical Gear Transmission System in Electric Vehicles with a Large Helix Angle," *Machines*, vol. 11, no. 7, pp. 1-2023. [CrossRef] [Google Scholar] [Publisher Link]

[55] Xiao Wu et al., "A Revised Method to Calculate Time-Varying Mesh Stiffness of Helical Gear," *MATEC Web of Conferences*, vol. 355, pp. 1-9, 2022. [CrossRef] [Google Scholar] [Publisher Link]

[56] Roee Cohen et al., "A Novel Method for Helical Gear Modeling with an Experimental Validation," *Nonlinear Dynamics*, vol. 112, pp. 1-19, 2024. [CrossRef] [Google Scholar] [Publisher Link]

[57] Iulian Lupea, Mihaiela Lupea, and Adrian Coroian, "Helical Gearbox Defect Detection with Machine Learning Using Regular Mesh Components and Sidebands," *Sensors*, vol. 24, no. 11, pp. 1-25, 2024. [CrossRef] [Google Scholar] [Publisher Link]

[58] Fei Liu et al., "Study on the Vibration Characteristics of Worm Helical Gear Drive," *Mechanism and Machine Theory*, vol. 191, 2024. [CrossRef] [Google Scholar] [Publisher Link]

Table 4. Intergeometry comparison of shortlisted casing configurations using modal and harmonic analysis results

		Existing Model (Rectangular Shape Top and Rectangular Shape Bottom)								*Modified Design I (Curved Shape Top and Rectangular Shape Bottom)*						*Modified Design II (Curved Shape Top and Curved Shape Bottom)*					
Thickness →		**5 mm**		**5 mm**		**7 mm**		**9 mm**		**5 mm**		**7 mm**		**9 mm**		**5 mm**		**7 mm**		**9 mm**	
Material →		**S.S.A36 (Current)**		**AISI 1050 H.C.S.**		**AISI 1050 H.C.S.**		**S.S.A36**		**S.S.A36**		**S.S.A36**		**S.S.A36**		**S.S.A36**		**AISI 1050 H.C.S.**		**AISI 1050 H.C.S.**	
Modal Analysis		***Freq (Hz)***	***Total Def. (mm)***	***Freq (Hz)***	***Total Def. (mm)***	***Freq (Hz)***	***Total Def. (mm)***	***Freq (Hz)***	***Total Def. (mm)***	***Freq (Hz)***	***Total Def. (mm)***	***Freq (Hz)***	***Total Def. (mm)***	***Freq (Hz)***	***Total Def. (mm)***	***Freq (Hz)***	***Total Def. (mm)***	***Freq (Hz)***	***Total Def. (mm)***	***Freq (Hz)***	***Total Def. (mm)***
		945.29	12.624	921.81	12.095	1069.8	12.419	1240.1	12.567	968.94	12.701	1140.5	12.012	1275.8	12.186	796.82	13.757	914.62	12.954	1016.9	12.449
		1797.7	23.367	1749.5	22.306	2033.2	22.134	2227.2	23.536	1840.9	24.285	2093.0	24.281	2286.0	24.027	1592.3	21.970	1733.6	19.595	1870.5	18.122
		2094.2	25.807	2041.1	24.808	2351.3	21.317	2597.0	17.460	2260.6	28.303	2491.0	22.576	2739.3	18.551	1942.5	15.093	2001.2	13.126	2065.7	12.183
		2952.8	16.630	2858.4	14.507	3078.8	12.454	3259.4	13.144	3012.6	15.291	3248.1	14.402	3352.6	13.395	2065.1	26.546	2282.4	19.876	2543.9	16.082
		2982.7	17.065	2894.5	17.532	3366.3	30.772	3312.2	23.872	3075.9	19.020	3309.6	21.200	3458.5	25.105	2743.8	21.455	2879.3	22.671	3081.5	25.762
		3384.3	65.388	3321.5	62.543	3954.3	43.850	4058.0	50.031	3451.0	72.674	3918.7	55.165	3944.3	53.174	3351.4	53.356	3575.4	33.306	3806.9	31.767
Harmonic Analysis	***Maximum Total Deformation (mm)***	0.003557		0.001960		0.002045		0.00108		0.00122		0.0006		0.00011		0.00569		0.0111		0.0025155	
	Maximum Equivalent Stress (MPa)	3.5147		2.0267		9.9441		4.9708		1.5295		2.8917		0.69203		21.051		137.45		28.103	

Note: *From the existing model, S.S.A36 9 mm was shortlisted; in the modified designs, S.S.A36 9 mm and 5 mm were considered in Design I and II respectively, with Modified Design I (S.S.A36 9 mm) finally selected in comparison with baseline model (S.S.A36, 5 mm).*

Table 6. Comparison of regression and ANN predictions with FEA Results for interpolated thickness levels (CTRB, S.S.A36, 9 mm)

Thickness (mm)	Ansys FEA results	Predicted Regression Analysis (RA)	Predicted Artificial Neural Network (ANN)	% Error (ANSYS and Predicted RA)	% Error (ANSYS and Predicted ANN)	Ansys FEA results	Predicted Regression Analysis (RA)	Predicted Artificial Neural Network (ANN)	% Error (ANSYS and Predicted RA)	% Error (ANSYS and Predicted ANN)
	TOTAL DEFORMATION (mm)					*EQUIVALENT VON MISES STRESSES (MPa)*				
5.5	0.0007745	0.0006775	0.0005950	12.53%	23.18%	4.1724	3.62998	3.2165664	13.00%	22.91%
6.0	0.0017444	0.0015460	0.0013801	11.38%	20.89%	4.6981	4.06640	3.9867531	13.45%	15.15%
6.5	0.0024666	0.0021011	0.0020401	14.82%	17.30%	4.8738	4.25999	3.5009666	12.60%	28.17%
7.5	0.0027138	0.0022711	0.0020993	16.32%	22.65%	4.6483	3.91871	3.6032348	15.70%	22.49%
8.0	0.0021934	0.0018860	0.0017197	14.02%	21.60%	3.9578	3.38384	2.9813129	14.51%	24.68%
8.5	0.0013730	0.0011875	0.0010473	13.52%	23.73%	3.1092	2.60614	2.1190365	16.18%	31.85%